



Modeling Earth's surface topography: decomposition of the static and dynamic components

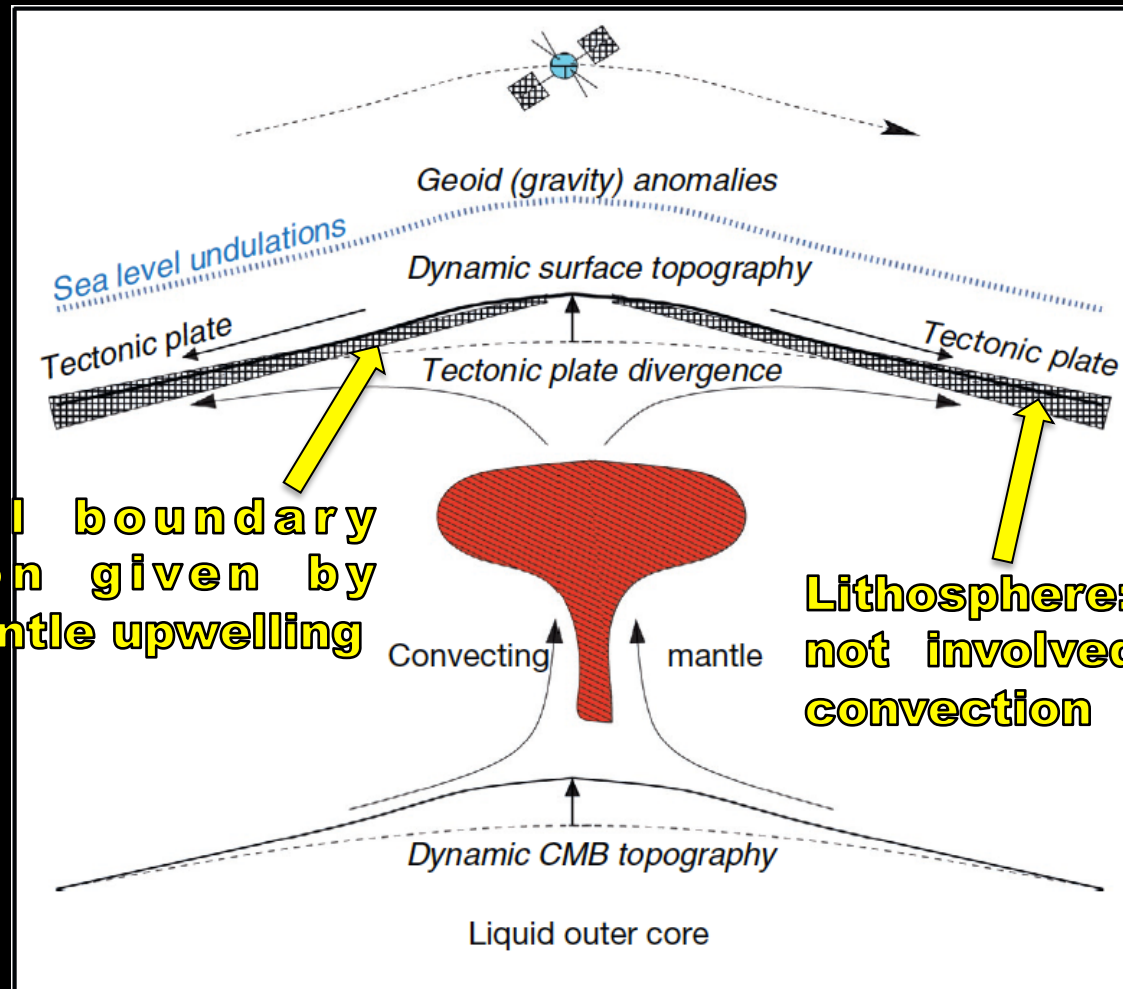
Mattia Guerri

***Københavns Universitet
Institut for Geovidenskab og Naturforvaltning***

Introduction

- **Can we separate the isostatic and dynamic component of topography?**
- **What are the uncertainties affecting the modeling of Earth's surface topography? What is their effect?**
- **Quantify the errors related to lithosphere density (crust + lithospheric mantle), mantle density, mantle viscosity.**

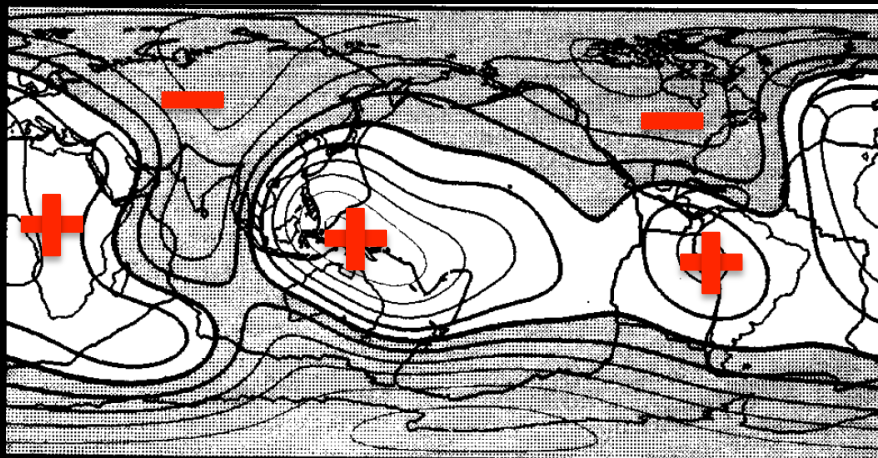
Dynamic topography



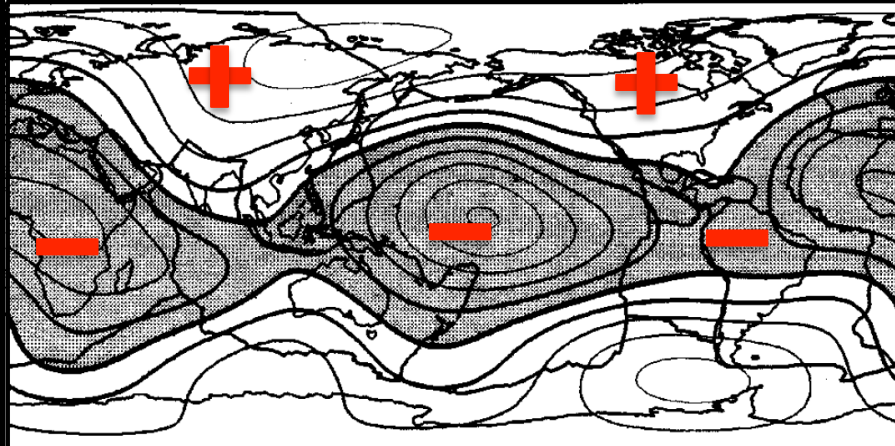
[modified from Forte et al. 2015]

Lower mantle heterogeneity, dynamic topography and the geoid [Hager et al. 1985]

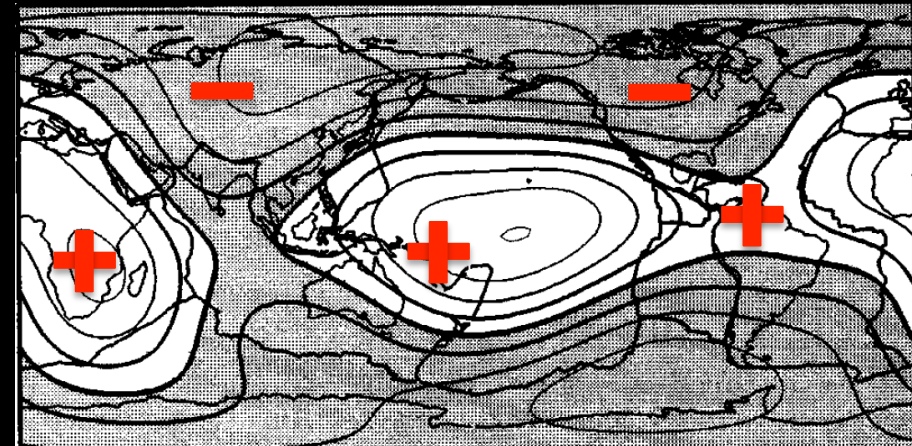
Observed geoid



Synthetic geoid, static Earth



Synthetic geoid, dynamic Earth



Modeling surface topography [Dynamic component]

To compute the dynamic component of topography we essentially need two elements:

- **Mantle density**



- **Mantle viscosity**



Modeling surface topography [Dynamic component]

Mantle density

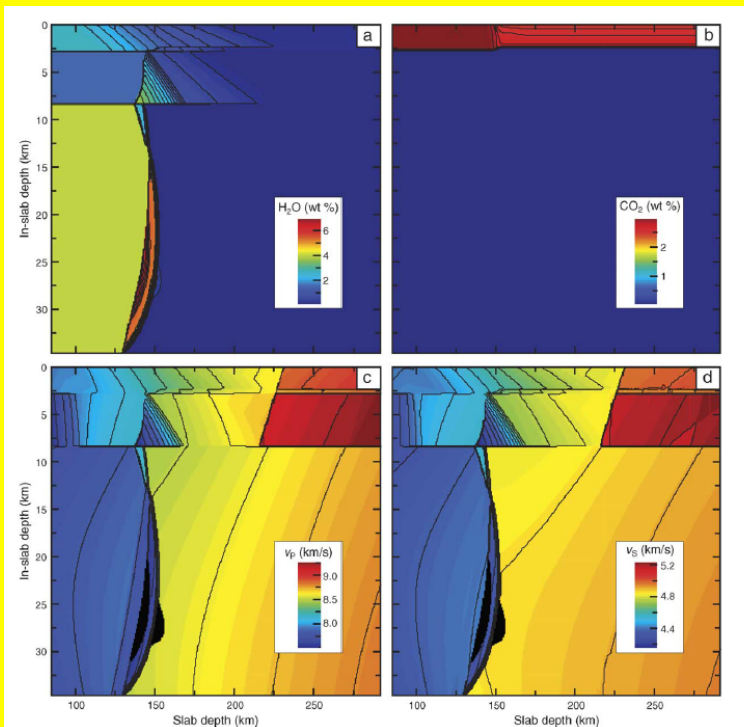
Inferred from models of seismic waves velocities using conversion coefficients:

- **Constant conversion coefficients, i.e.**
 $d\ln\rho/d\ln V_s = 0.2 \mid 0.4$.
- **1D profiles based on mineral physics constraints.**
- **3D structures from joint inversion of seismic and geodynamic constraints.**
- **P-T-C dependent distributions from conversion of velocity to density using thermodynamic modeling.**

Forward modeling of mantle physical properties

Compute mantle rock physical properties as a function of pressure and temperature starting from an input composition.

**Thermodynamic modeling code:
Perple_X [Connolly, 2009].**



Forward modeling of mantle physical properties

How Perple_X works:

- **minimization of the Gibbs free energy of the system to compute identify amount and composition of the stable mineral phases.**
- **Computation of High P-T rock physical properties applying EOSs and starting from a database of thermoelastic mineral properties.**
- **Several thermodynamic properties datasets are implemented in Perple_X.**

Forward modeling of mantle physical properties

Thermodynamic formalism and thermoelastic properties database from Stixrude and Lithgow-Bertelloni [2005, 2011].

1] Fundamental thermodynamic relations:

$$\frac{\partial^3 G}{\partial P \partial V \partial T} = \frac{\partial}{\partial T} \left(\frac{V}{K} \right)_P$$

2] Euler Form.

3] Legendre transformations.

$$G(P, T) = F(V, T) + PV(P, T)$$

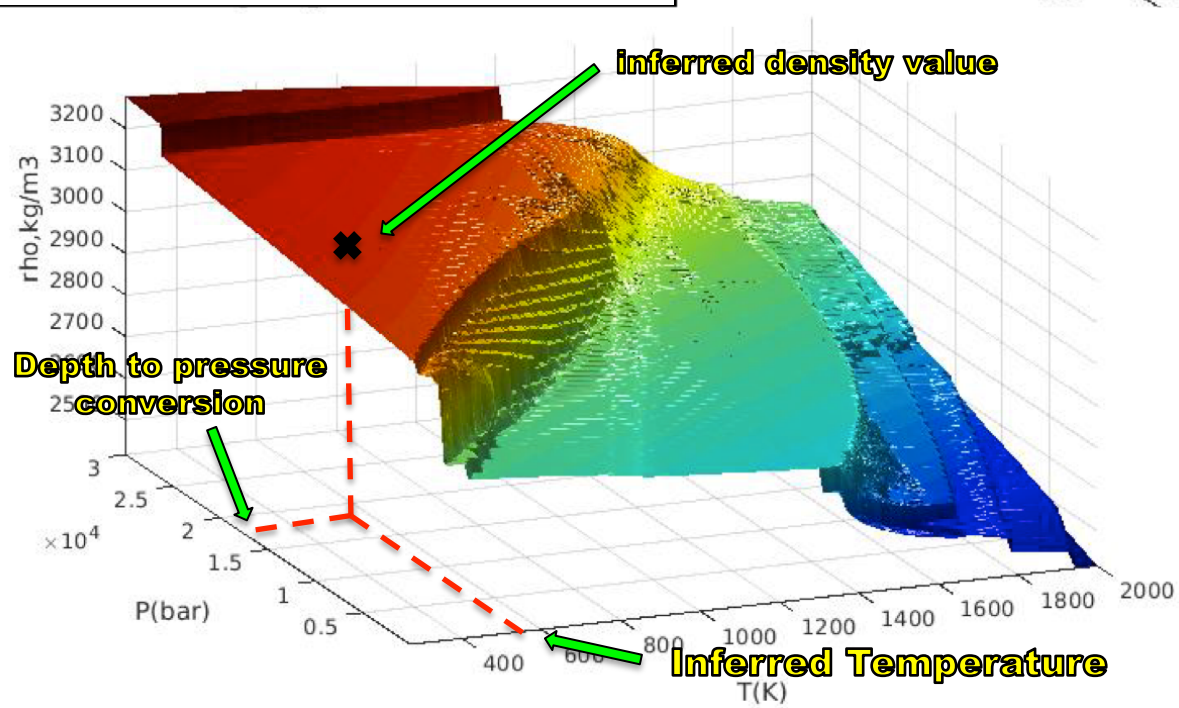
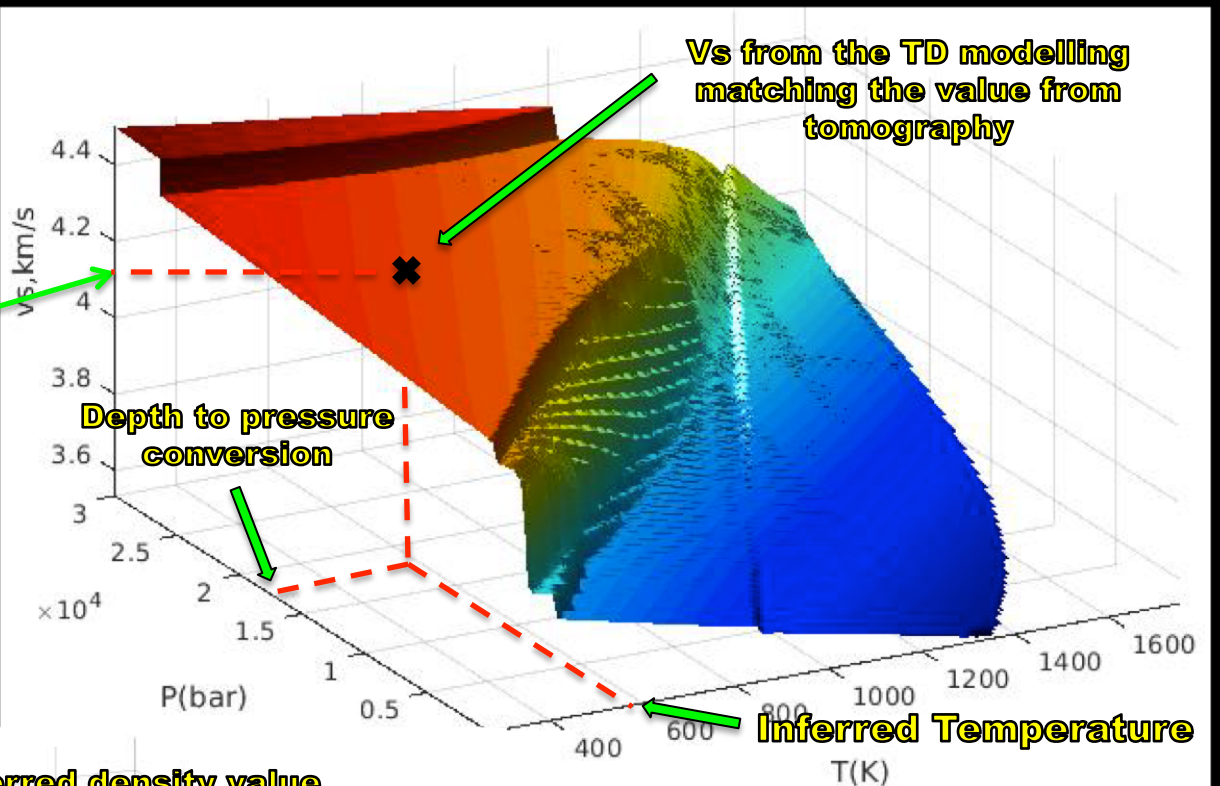
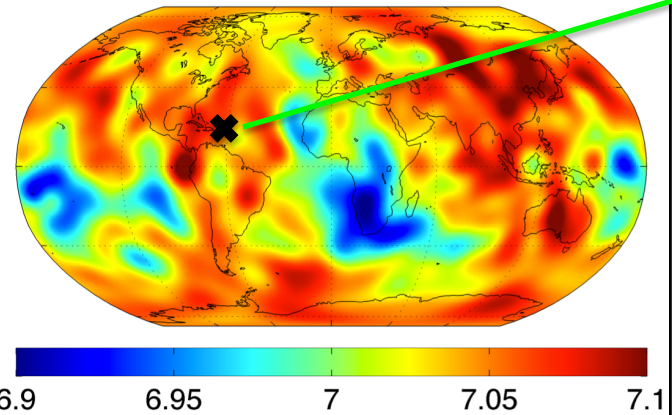
4] Anisotropic generalization

$$\sigma_{ij} = -P\delta_{ij} + \tau_{ij}$$

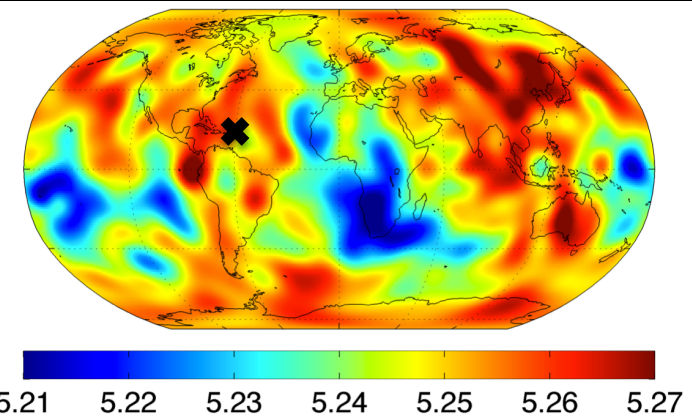
Converting seismic wave speed in density

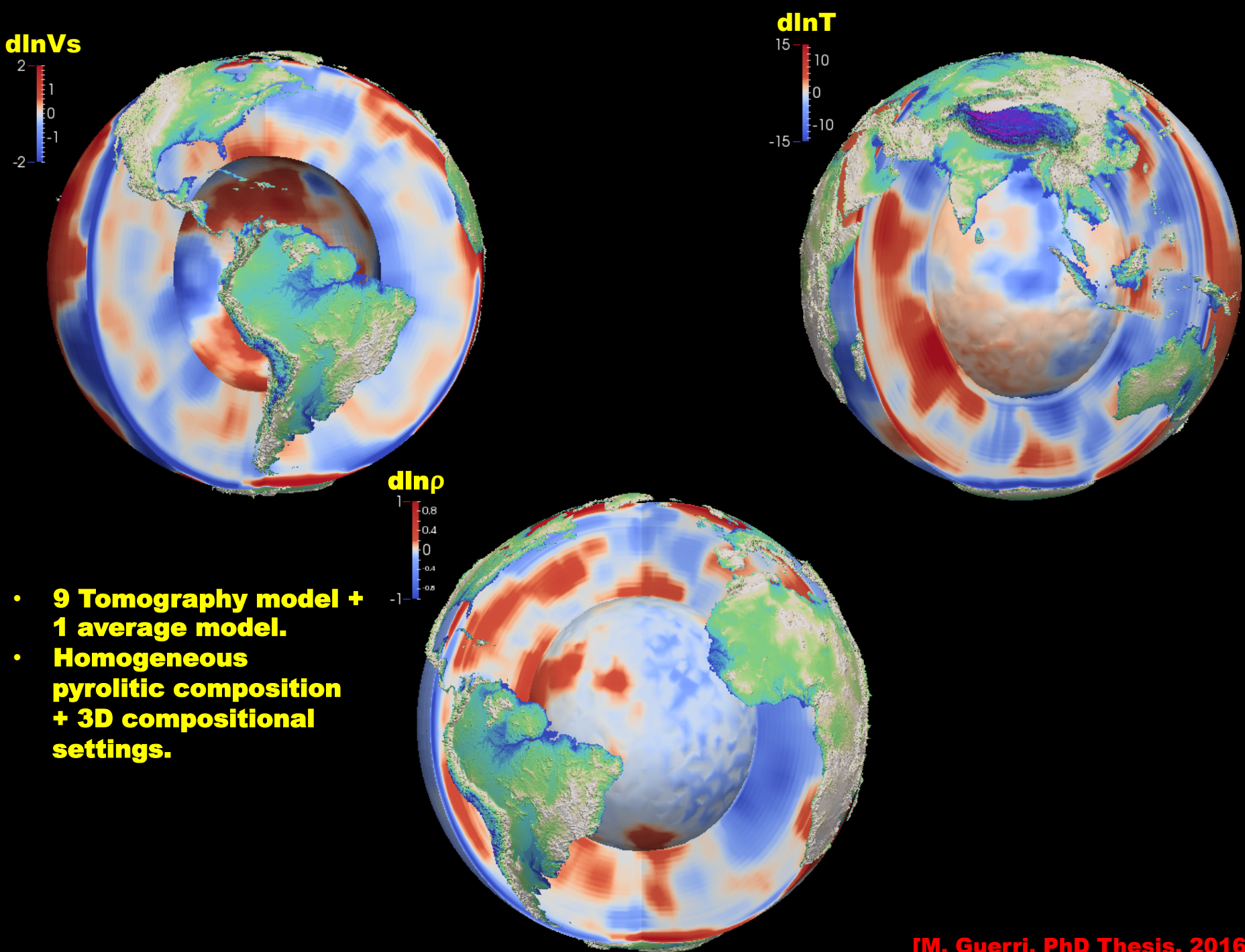
Vs at 2250 km

model SPani [Tesoniero et al. 2015]



Inferred density at 2250 km, pyrolytic comp.





Modeling long wavelength surface topography

[Dynamic component]

- **Mantle density**



- **Mantle viscosity**



Inferring mantle viscosity

Mitrovica and Forte [2004]: viscosity inference through joint inversion of GIA and surface observables linked to mantle convection.

GIA: glacial isostatic adjustment.

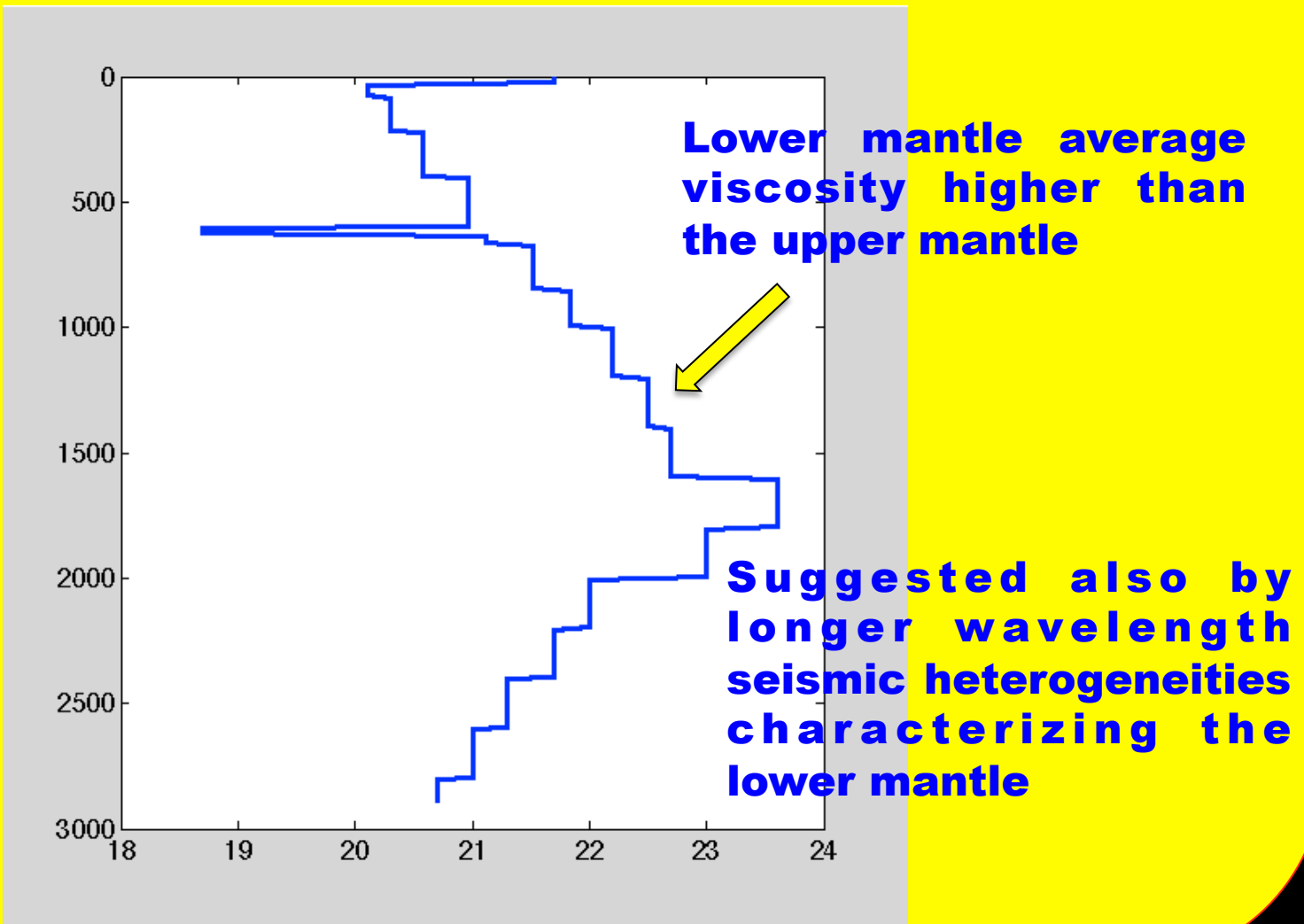
- Depth sensitivity varies (until a depth of ~1500 km).
- Insensitive to the deeper portion of the mantle.

Convection related observables: free-air gravity anomaly, excess ellipticity of the CMB, tectonic plate divergence.

- Depth sensitivity is a function of the viscosity structure itself.
- Insensitive to absolute viscosity value (except plate velocities).

Inferring mantle viscosity

V1 viscosity profile (Mitrovica and Forte, 2004).



Inferring mantle viscosity

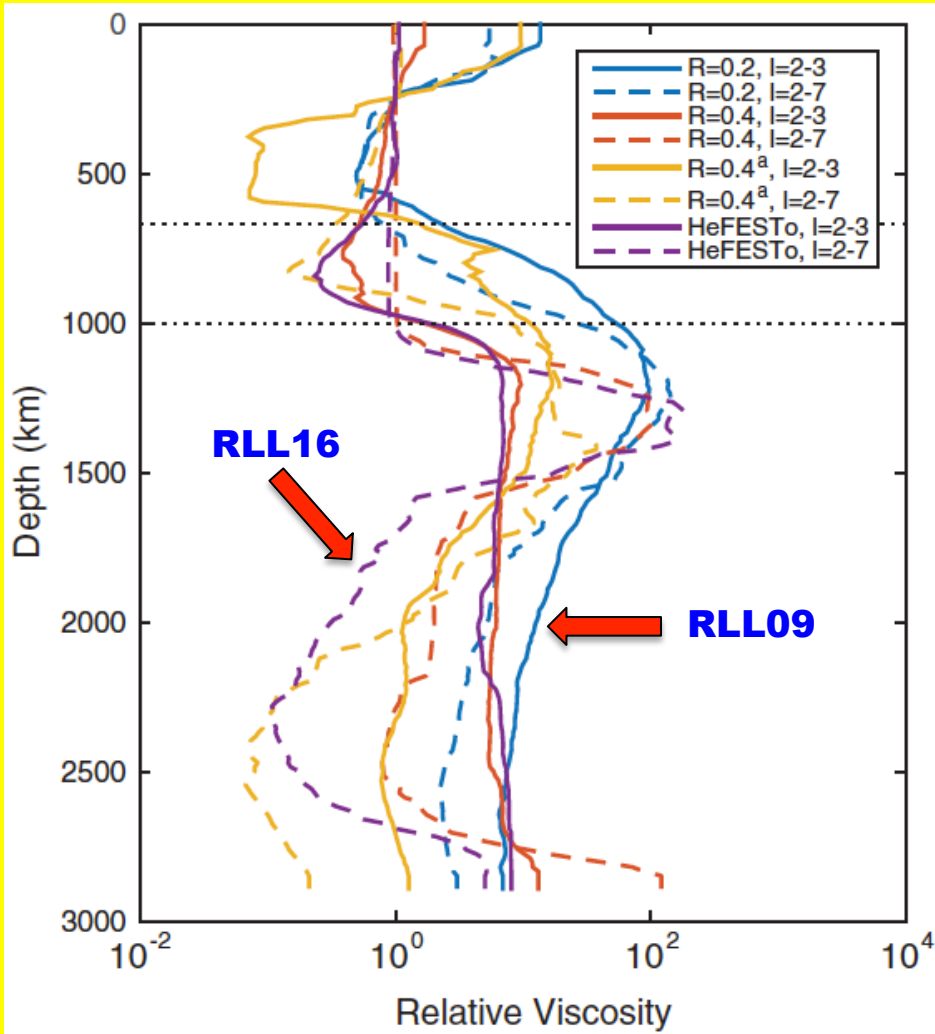
Rudolph et al. [2015]: inversion (Bayesian approach) of the long-wavelength geoid. Starting density models inferred from a tomography model (SEMUCB-WM1, French and Romanowicz [2014]).

Conversion of seismic velocity to density:

- **constant conversion coefficients**
- **look up table procedure from thermodynamic modelling results obtained with HEFESTO [Stixrude and Lithgow-Bertelloni, 2007].**

Inferring mantle viscosity

Rudolph et al. [2015] viscosity profiles.



Inferring mantle viscosity

3D P-T dependent viscosity model.

$$\varepsilon'_{diff} = A_1 d^{-p_1} \sigma \exp\left(-\frac{E_1 + pV_1}{RT}\right)$$

$$\varepsilon'_{dis} = A_3 \sigma^{n_3} \exp\left(-\frac{E_3 + pV_3}{RT}\right)$$

Upper mantle: parameters from Korenaga and Karato [2008] inferred through Bayesian inversion of experimental data.

Lower mantle: parameters from Yamazaki and Karato [2001]. Perovskite governed rheology.

Modeling dynamic surface topography

- **Mantle density** 
- **Mantle viscosity** 

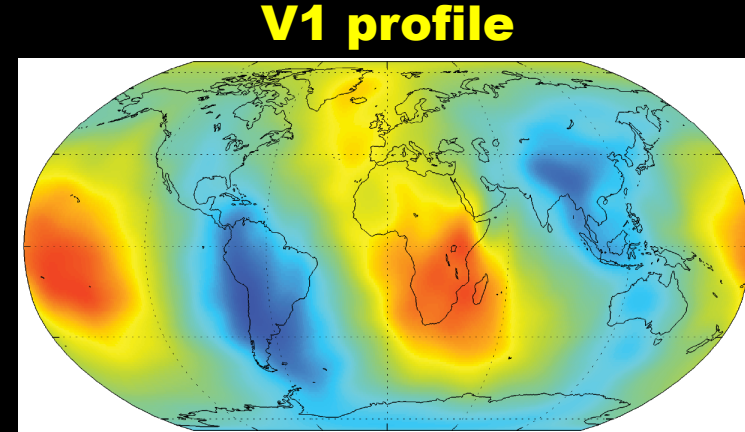
**Dynamic topography computation performing
Instantaneous mantle flow modeling**

StagYY [Tackley, 2008]

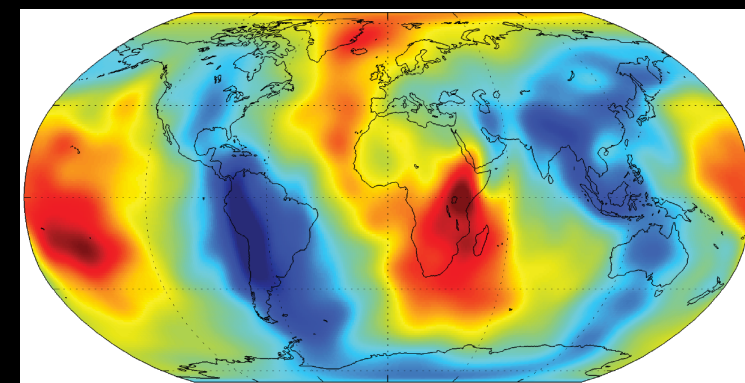
- **compressible mantle**
- **Large variations in viscosity**
- **3D spherical shell (Yin-Yang grid)**

Modeling surface dynamic topography

Mean model converted in density with a homogeneous pyrolitic composition.



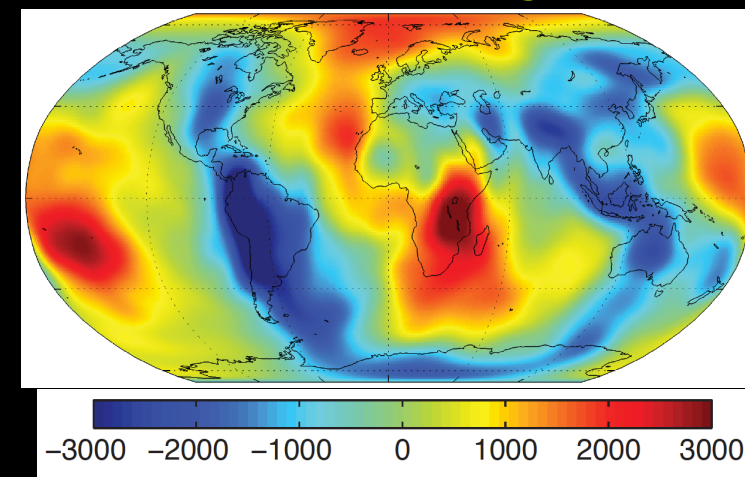
RLL16



3D viscosity

Dynamic topography pattern dominated by LLSVPs in the lower mantle and slabs.

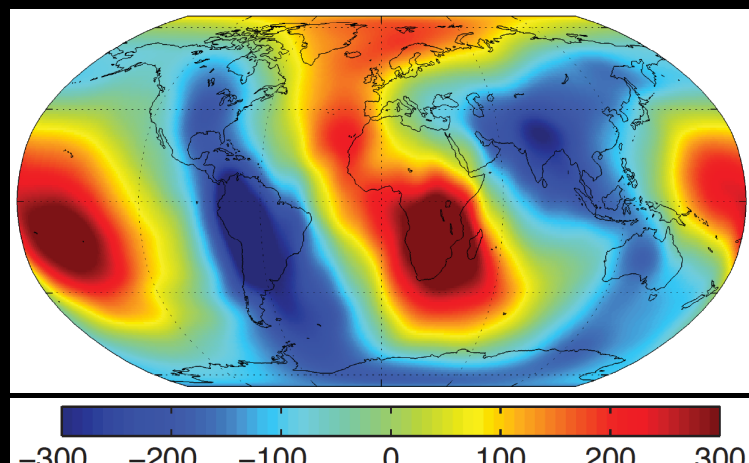
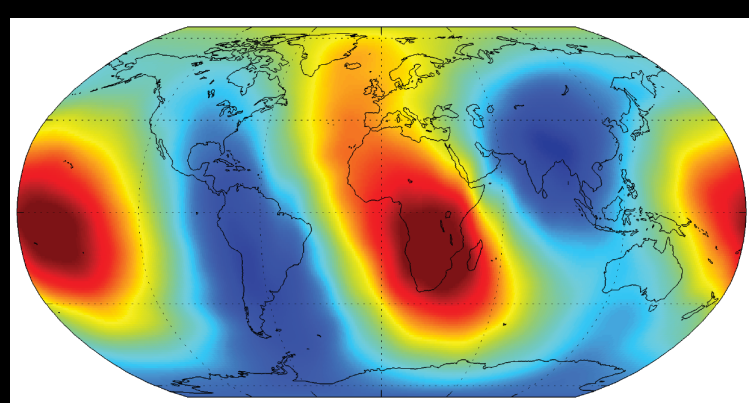
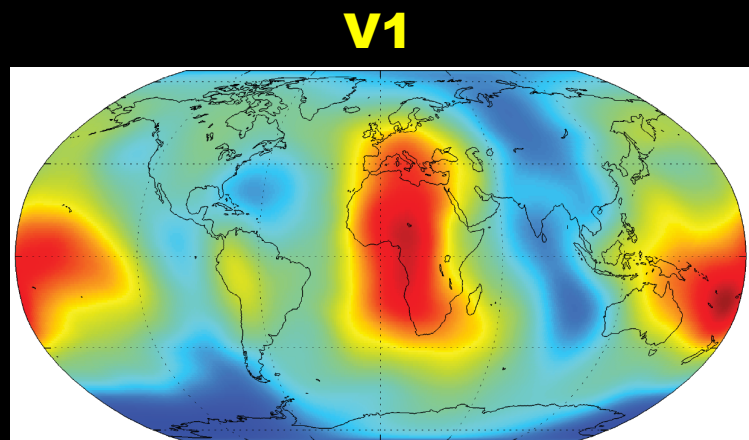
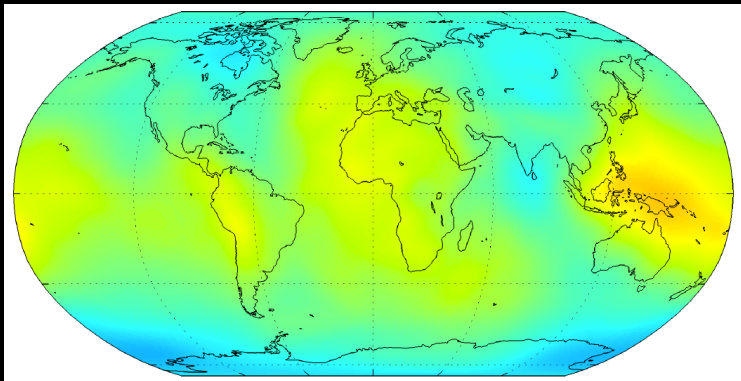
Strong dynamic topography amplitude (>4km), regardless of the employed viscosity structure.



Associated synthetic geoid

- Fundamental in order to further investigate the reliability of the obtained dynamic topography model.
- At long wavelength the geoid is dominated by anomalies in the deep mantle and large scale deformation of the boundaries (surface and CMB).
- Strong undulation amplitude (>400 m).

Observed geoid



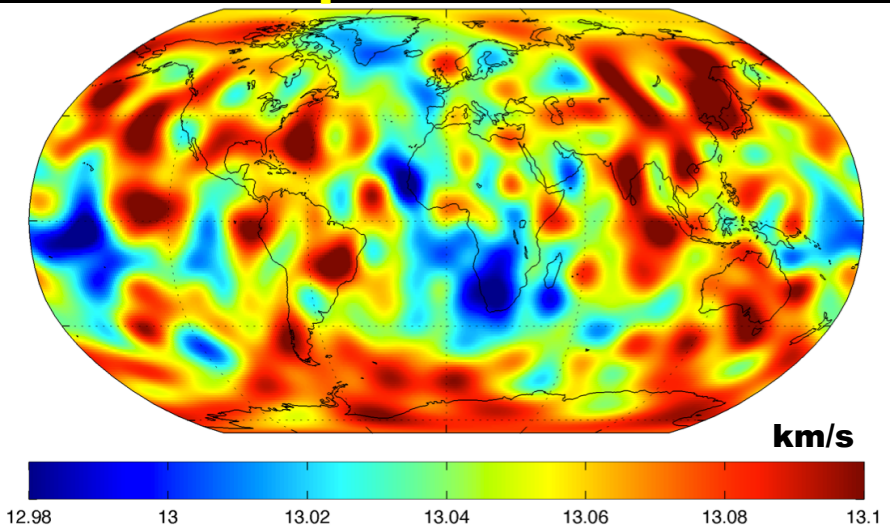
Modeling dynamic surface topography

- **Absolute velocity values from the seismic tomography models.**
- **Uncertainties affecting forward modeling of mantle mineralogy and physical properties.**
- **Mantle viscosity structure. Although we test several proposed viscosity structures.**
- **Mantle chemical heterogeneities.**

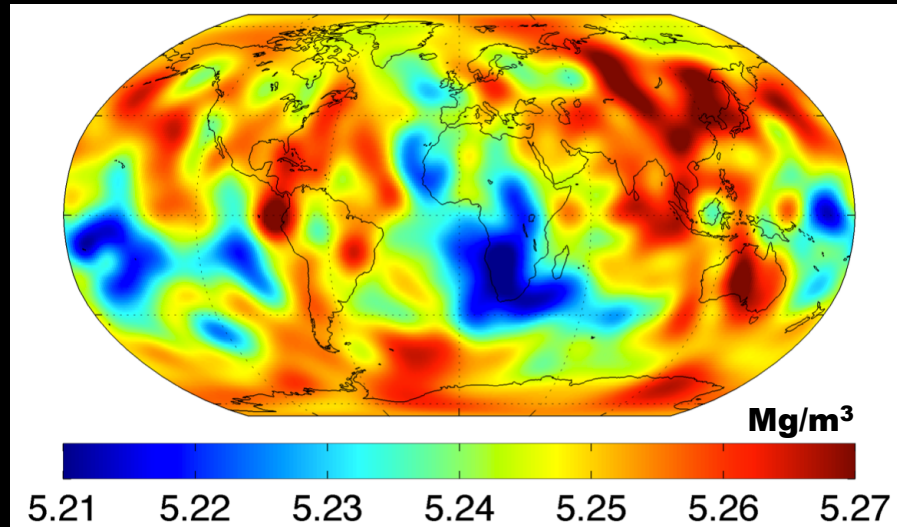
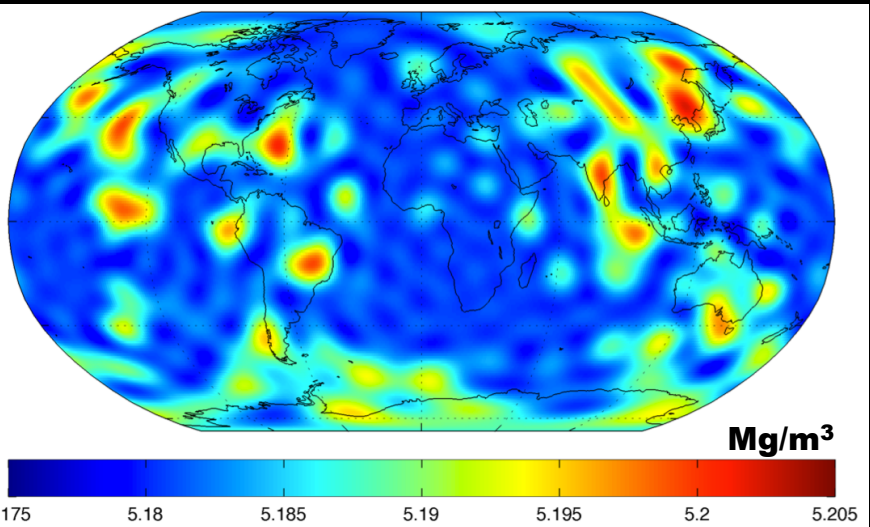
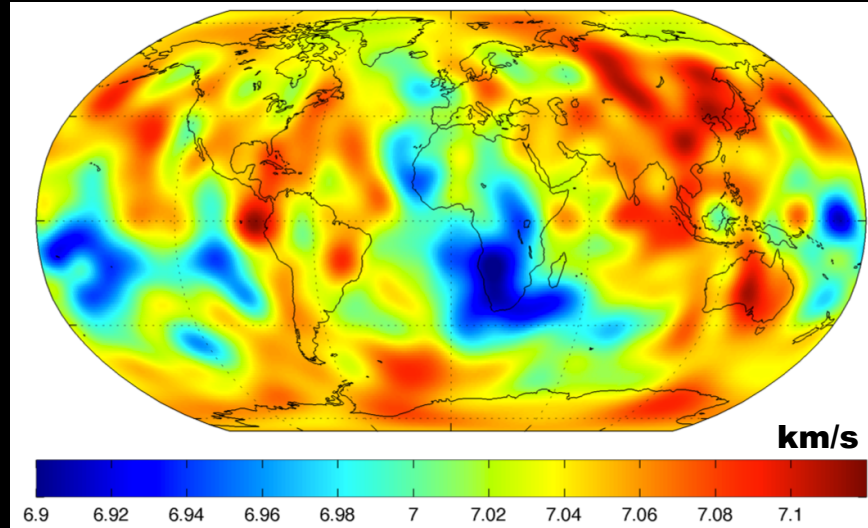
Inferring density, Vp vs. Vs tomography models

Spani [Tesoniero et al. 2015]

Vp at 2250 km

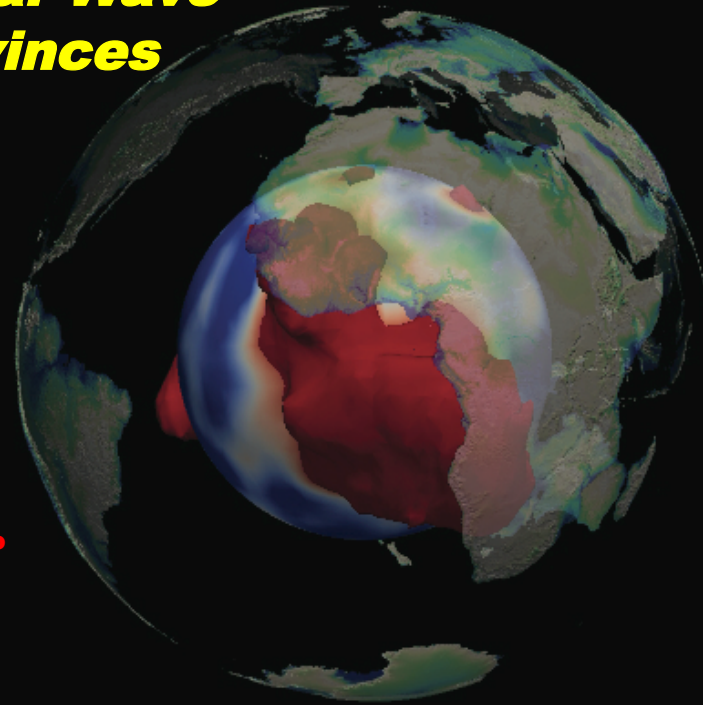
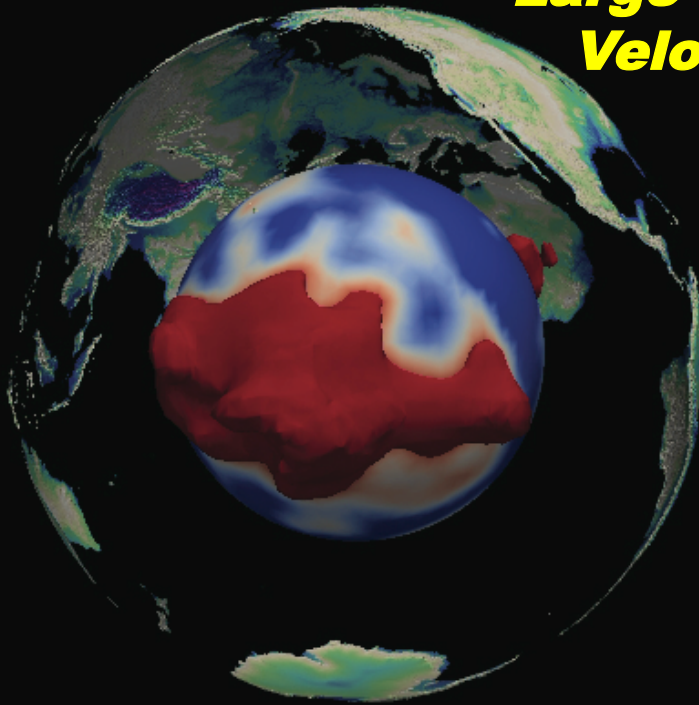


Vs at 2250 km



Modeling the dynamic component

**Large Low Shear Wave
Velocity Provinces**



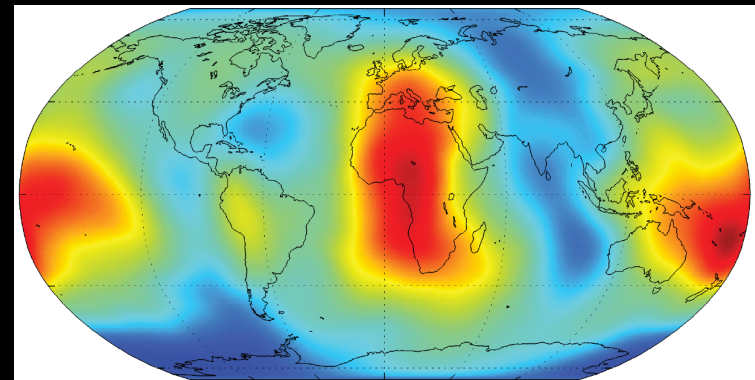
A purely thermal interpretation leads to density anomalies generating strong deformation at the surface.

Chemical heterogeneity is required to satisfy both seismic and geodetic data.

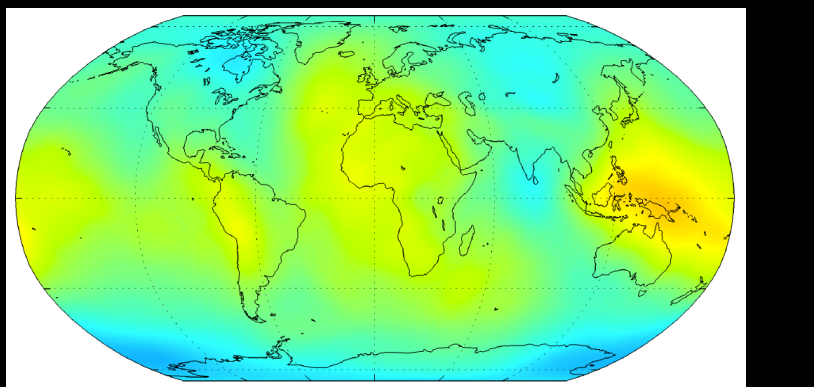
Modeling the dynamic component

- Iron enriched composition in the LLSVPs.
- Mg# decreased from 89 to 87.
- Better agreement with geoid amplitude keeping a good correlation coefficient.

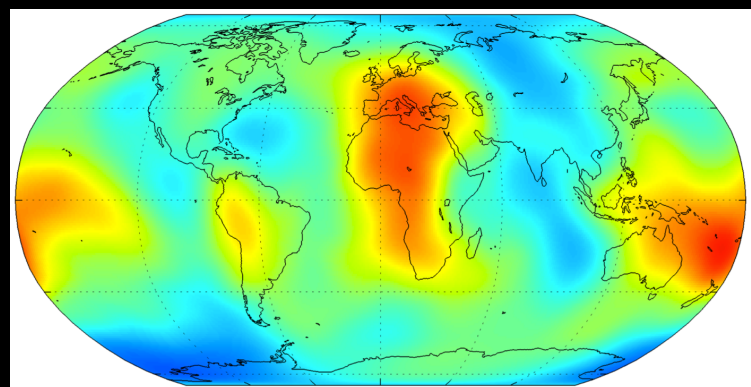
**Homogeneous comp.
Mg#89, cor. coef. = 0.82**



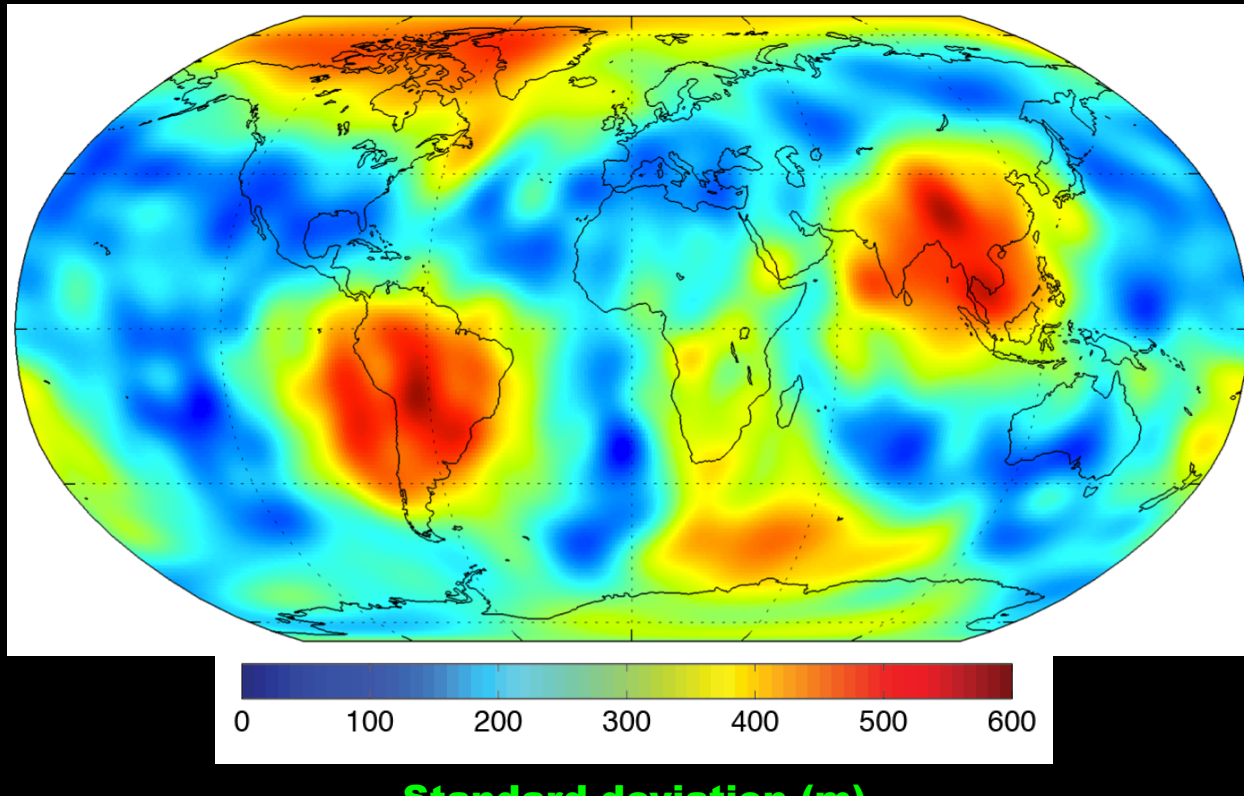
Observed geoid



**Modified pyrolite in LLSVP
Mg#87, cor. coef. = 0.80**

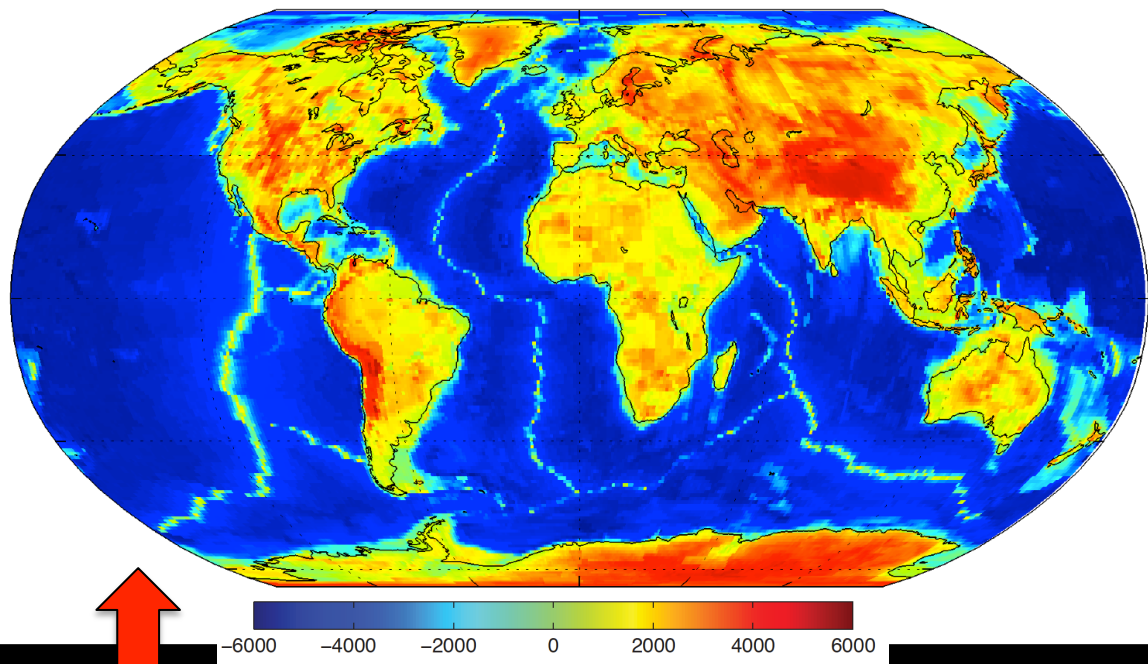


Modeling the dynamic component



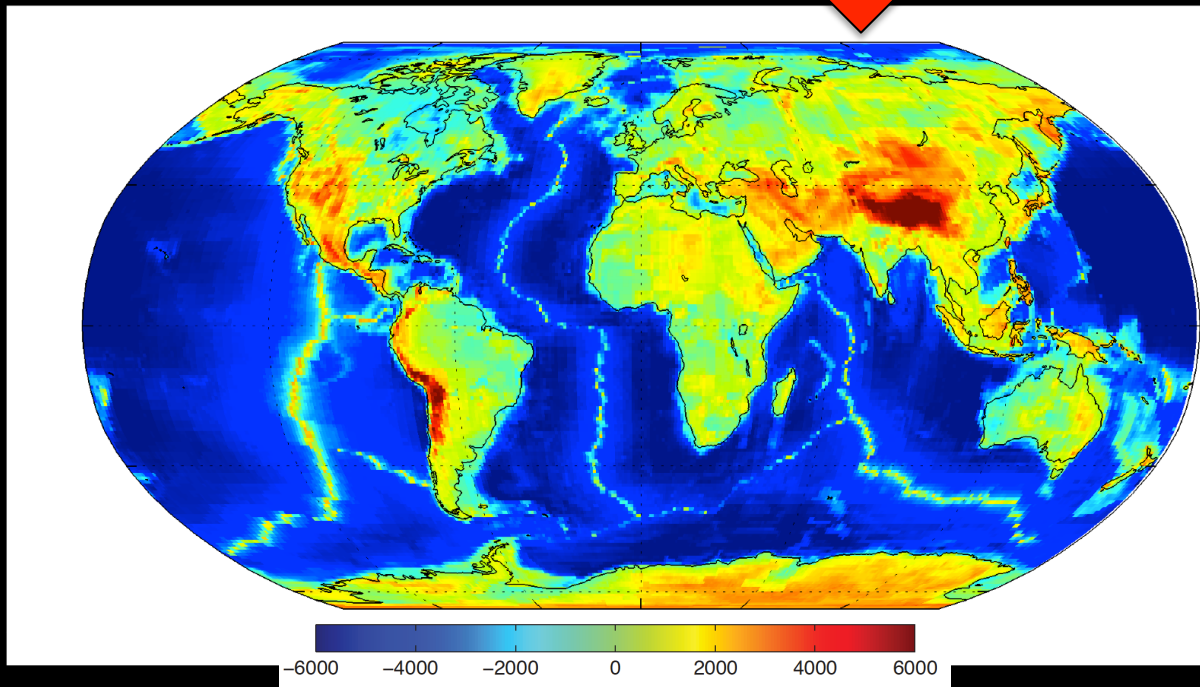
- **9 mantle density models.**
- **Homogeneous composition (pyrolite).**
- **Same viscosity profile (V1, Mitrovica and Forte [2004])**

Modeling the isostatic component

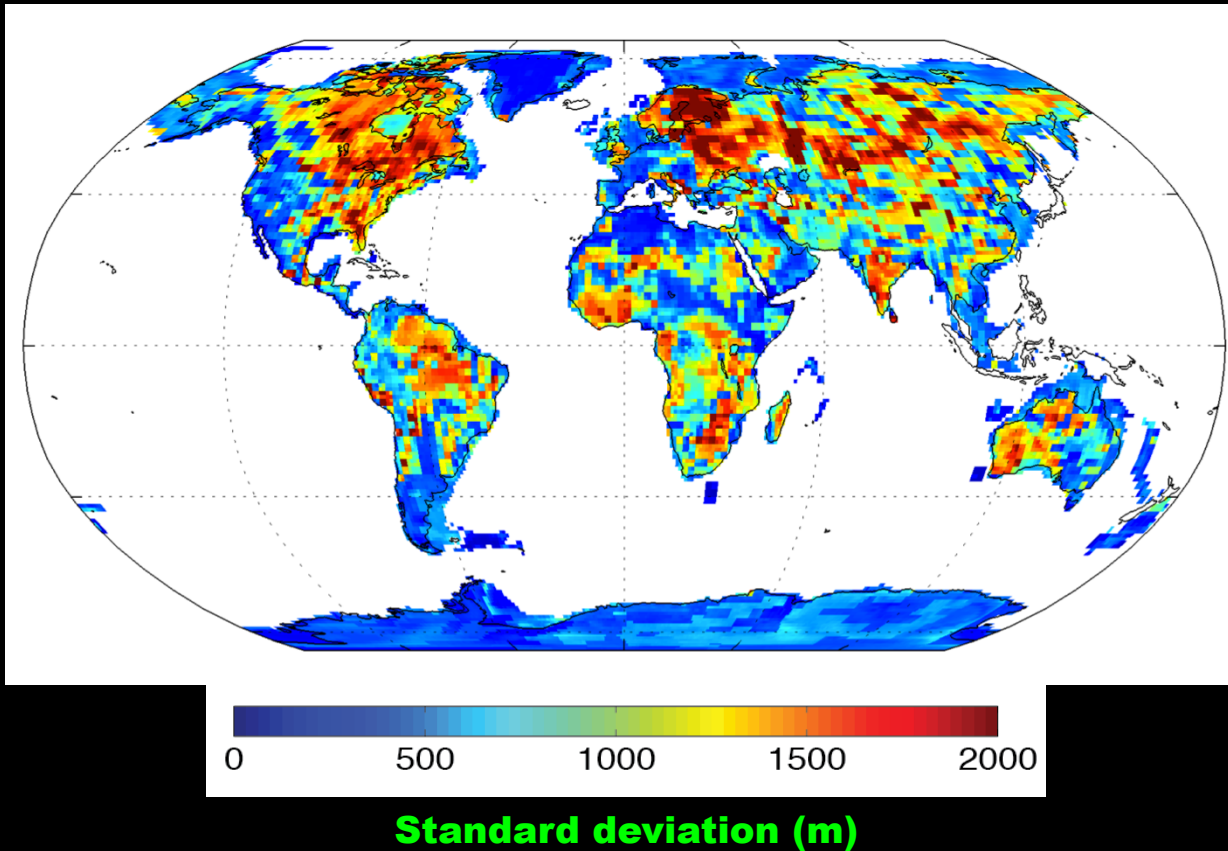


Crustal effect only

Crust + lithospheric mantle

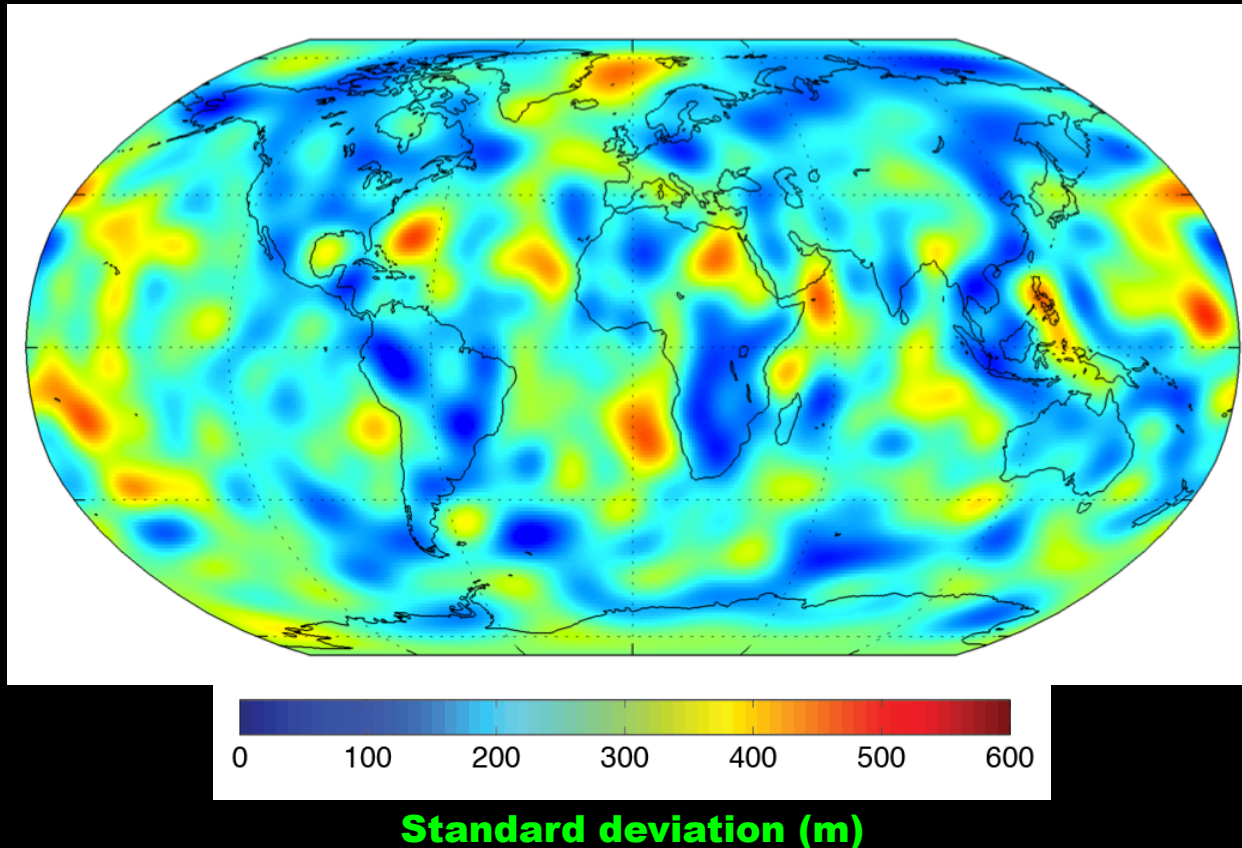


Modeling the isostatic component



- **11 crustal density models, Guerri et al [2015] + Crust 1.0 (Laske et al., 2013).**
- **3 chemical compositions + 2 different amount of water.**
- **2 methodological approach (forward and converted models).**

Modeling the isostatic component

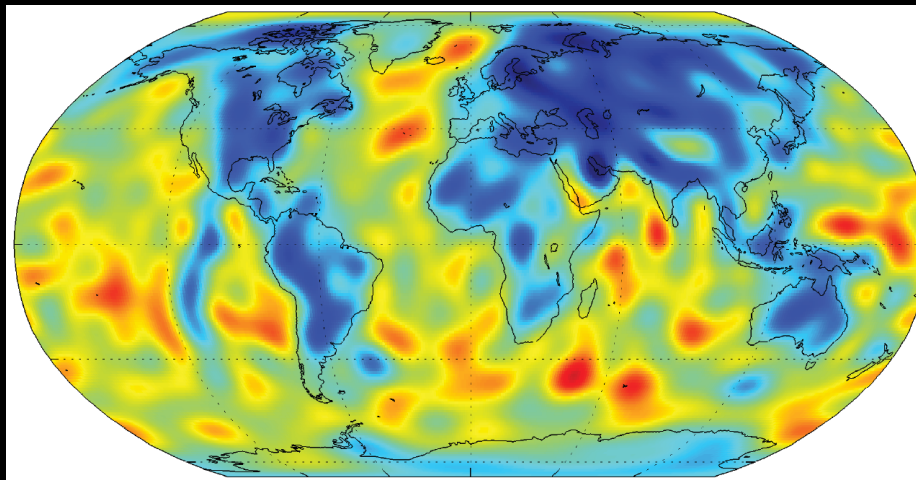


- **9 lithospheric mantle density models.**
- **Constant lithospheric mantle composition, pyrolite and harzburgite.**
- **Same crustal model.**

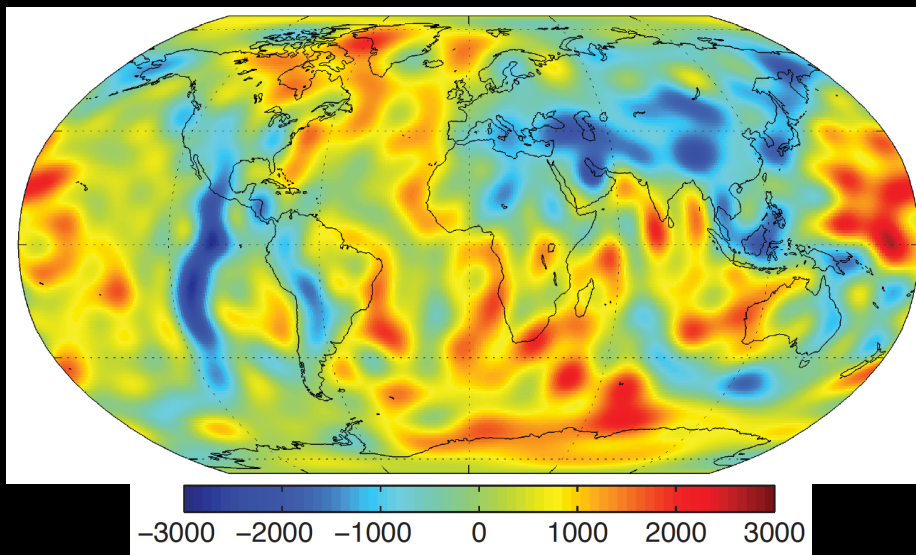
Residual topography maps

**Difference between observed and computed
isostatic topography**

Removing the crustal effect only



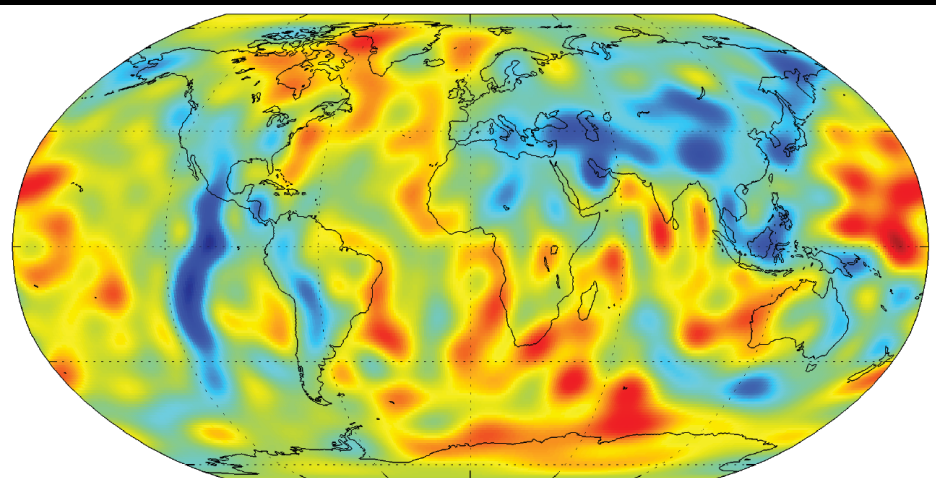
Removing the effect of the entire lithosphere



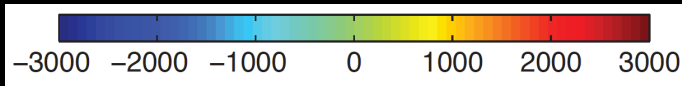
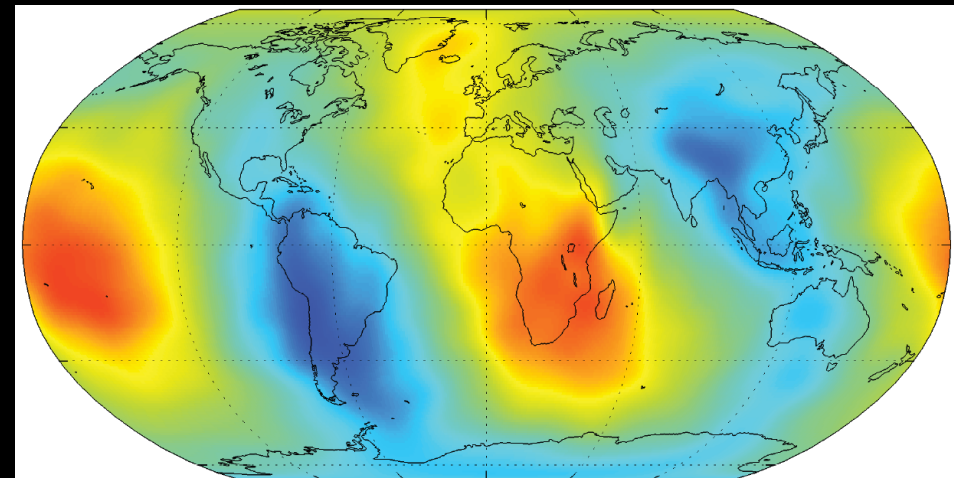
-3000 -2000 -1000 0 1000 2000 3000

Residual topography vs. Dynamic topography

Residual topography



Dynamic topography



Correlation coefficient = 0.31

Conclusion

- **Dynamic topography: strong elevated peak-to-peak values (>2km), unconstrained by geodetic observation.**
- **Dynamic topography: long wavelength pattern is well constrained but the amplitude is affected strong (10^2 m) uncertainties.**
- **Crustal models need to be constrained with other geophysical data (gravity constraints).**
- **Residual topography maps are strongly affected by isostatic component uncertainties, thus not representing a reliable estimate of dynamic topography.**

Thermodynamic framework

Gibbs free energy of the multi-phase assemblage:

$$G(\sigma_{ij}, T, n_\beta) = \sum_\beta n_\beta \mu_\beta(\sigma_{ij}, T, n_\beta)$$

$$\sigma_{ij} = -P\delta_{ij} + \tau_{ij}$$

Thermodynamic framework

Bulk and shear moduli computation
Third order Birch-Murnaghan equation of state
[modelling the effect of pressure]

Bulk modulus

$$K = (1 + 2f)^{5/2} \left[K_0 + (3K_0 K'_0 - 5K_0) f + \frac{27}{2} (K_0 K'_0 - 4K_0) f^2 \right]$$

Shear modulus

$$G = (1 + 2f)^{5/2} \left[G_0 + (3K_0 G'_0 - 5G_0) f + \left(6K_0 G'_0 - 24K_0 - 14G_0 + \frac{9}{2} K_0 K'_0 \right) f^2 \right]$$

$$-\eta_s \rho \Delta U_q$$

Thermodynamic framework

Eulerian finite strain formulation

Bulk modulus

$$K = (1+2f)^{5/2} \left[K_0 + (3K_0 K'_0 - 5K_0) f + \frac{27}{2} (K_0 K'_0 - 4K_0) f^2 \right] +$$

$$(\gamma + 1 - q) \gamma \rho \Delta U_q - \gamma^2 \rho \Delta (C_V T)$$

Shear modulus

$$G = (1+2f)^{5/2} \left[G_0 + (3K_0 G'_0 - 5G_0) f + \left(6K_0 G'_0 - 24K_0 - 14G_0 + \frac{9}{2} K_0 K'_0 \right) f^2 \right]$$

$$- \eta_s \rho \Delta U_q$$